J. Mar. Biol. Ass. U.K. (2007), **87**, 69–76
Printed in the United Kingdom
doi: 10.1017/S0025315407054835

Comparative morphometry of odontocete ears through computerized tomography

M. Morell*, E. Degollada*, M. van der Schaar*, J.M. Alonso*, E. Delory*, A. López†, A. Dewez‡ and M. André*ʃ

*Laboratori d'Aplicacions Bioacústiques (LAB), Universitat Politècnica de Catalunya, Spain. †Coordinadora para o Estudio dos Mamíferos Mariños (CEMMA), Spain. ‡Groupe d'Étude de la Faune Marine Atlantique (GEFMA), France. ʃCorresponding author, e-mail: michel.andre@upc.edu

Describing the auditory periphery of odontocetes is a key conservation issue to further assess the effect of acoustic pollution. Because all odontocetes produce species-specific frequency ranges, differences in echolocation signals should reflect anatomical differences in the auditory pathways. Here, we studied the ears of 15 odontocete species through 3D reconstructions from computerized tomography scans to extract standard measurements (bullae lengths/volumes and cochlear volume) and investigate the discriminatory weight of each of these variables as well as their relation to the species' hearing specificity. Any of the measurements appeared to be a good indicator of the species and could therefore be used to classify them. All the ear lengths and most volumes were strongly linearly correlated ($r > 0.9$) in all species and the proportion between the tympanic and periotic bones appeared to remain constant. This constant ratio could be an indication of a functional relationship between both structures, and might suggest an active role of the odontocete middle ear during target acoustic detection, providing new information on the odontocete sound reception mechanism. Our results are generally consistent with previous studies, although here the coefficients of correlation between animal lengths and the total volume and lengths of the bullae were lower ($0.77 < r < 0.86$), indicating that the length of the animals may not be a primary parameter to take into account when defining ear measurements. These results suggest that the measurements described characterize standard ears which could be used as a morphological basis for further species-specific acoustic comparison.

INTRODUCTION

While there is increasing concern about the impact of noise on cetaceans, very little is known on the species' hearing capabilities and acoustic pathway functionality.

The cetacean auditory system is characterized by a series of unique morphological adaptations. Amongst them, the frequency sensitivity of the hearing system is directly and evolutionarily related to the habitat use, and thus characterizes every cetacean species (Ketten & Wartzok, 1990).

In odontocetes, the external auditory meatus is occluded, mostly filled with cellular debris (Fraser & Purves, 1960) and is thought to hardly play any role in sound perception (Bullock et al., 1968). The middle and inner ear are enclosed by the tympanic and periotic bones respectively, forming the tympanic-periotic (T-P) complex. The T-P complex, which is suspended through ligaments outside the skull in a peribullar cavity, is surrounded by air sinuses that help accomplish an acoustic separation from the rest of the skull (Reysenach de Haan, 1957; Ketten & Wartzok, 1990; Nummela et al., 1999b).

The first comparative studies on cetacean ears were presented by Fraser & Purves (1960) who focused on the aerial sinuses, concluding that the configuration of the ventral aspect of cetacean skulls together with the air space development provided a guide to the systematic classification of the order Cetacea. Wever et al. (1971a, b and c) were amongst the first to study the morphology of the dolphin cochlea. They centred their analysis on the description of the basilar membrane, the hair and ganglion cells and stated that the inner ear anatomy was consistent with the extension of sensitivity towards very high frequencies.

Electrophysiological methods allowed McCormick et al. (1970) to hypothesize on the role of bone conduction in dolphin hearing. Ridgway (1983) studied the sound reception at the cochlea, the production of sound in the nasal system, and attempted to test the dolphin capability for phase detection using the auditory brainstem response (ABR) technique.

The use of images (computerised tomography scans and magnetic resonance imaging) and the possibility of three-dimensional reconstructions opened a new research window. Through image diagnosis techniques, Ketten & Wartzok (1990) and Ketten (1992, 1994) divided odontocetes into two groups according to their acoustic production capabilities: type I included species with echolocation pulse peak frequency over 100 kHz and type II, under 100 kHz. Interestingly, the cochlear morphometry was significantly different between these two groups, especially the spiral geometry and basilar membrane stiffness: species whose hearing was adapted to very high frequency resolution presented a thicker membrane. They also stated that bullae

Table 1. *Known audiograms of some species.*

Species	Frequency range (kHz)	Maximum sensitivity (kHz)	Reference
*Stenella coeruleoalba**	0.5–160 (B)	64 (B)	Kastelein et al., 2003
*Delphinus delphis**	11–152 (E)	60–70 (E)	Popov & Klishin, 1998
*Tursiops truncatus**	5–140 (E)	80 (E)	Popov & Supin, 1990a
	0.075–150 (B)	45 (B)	Johnson, 1967
*Phocoena phocoena**	10–160 (E)	30 and 125 (E)	Popov et al., 1986
	0.25–180 (B)	100–140 (B)	Kastelein et al., 2002
Orcinus orca	1.2–120 (E)	20 (E)	Szymanski et al., 1999
	4–120 (B)	12–20 (B)	Hall & Johnson, 1971
Delphinapterus leucas	~16–110 (E)	60–80 (E)	Popov & Supin, 1987; Klishin et al., 2000
	1–120 (B)	~30 (B)	White et al., 1978; Awbrey et al., 1988; Johnson, 1992
Inia geoffrensis	8–120 (E)	20–25 and 70–80 (E)	Popov & Supin, 1990b
	1–100 (B)	12–64 (B)	Jacobs & Hall, 1972
Pseudorca crassidens	2–115 (B)	16–64 (B)	Thomas et al., 1988
Grampus griseus	1.6–110 (B)	8–64 (B)	Nachtigall et al., 1995
Lipotes vexillifer	1–200 (B)	16–64 (B)	Wang et al., 1992
Lagenorhynchus obliquidens	0.10–140 (B)	64 (B)	Tremel et al., 1998
Tursiops gilli	2–135(B)	30–80 (B)	Ljungblad et al., 1982
Sotalia fluviatilis	4–135 (B)	85 (B)	Sauerland & Dehnhardt, 1998

*, species described in our study; E, electrophysiological audiogram; B, behavioural/psychophysical methods.

dimensions and cochlear lengths were strongly correlated with animal size ($0.8< r <0.95$), but no correlation was found between basilar membrane length and frequency.

The role of the cetacean middle ear is poorly understood and some authors have even expressed doubts about its functionality (e.g. Fraser & Purves, 1954; Reysenbach de Haan, 1957; McCormick et al., 1970; Fleischer, 1978; Ridgway et al., 1997). Nummela et al. (1999a, 1999b) and Hemilä et al. (1999, 2001) presented several studies that brought data on the middle ear function during sound transmission. They observed isometric scaling in odontocetes and proposed a model which would explain an increase of the vibration velocity at the oval window level and would consider the vibration transfer from the tympanic plate to the oval window. The model was validated with audiograms from different species.

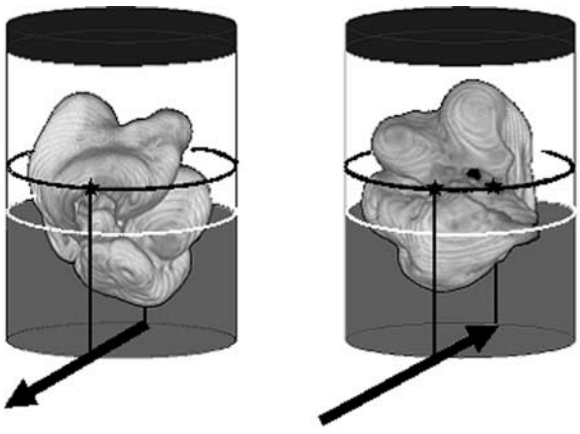

Figure 1. Standardized position of the ear for the CT scan. Three reference points were dye-marked on the same plane in all the samples (indicated with a star in the figure). The ears were placed in transparent plastic jars following a reference horizontal dotted line and held by a rigid polyurethane foam. This material presents the advantage of being almost transparent to the X-rays and of allowing the adjustment and moulding of the bullae. Once they were fixed, the jar was marked with two vertical lines passing by two of these three points to orientate the samples on the scanning table reference marks. The arrow shows the scan orientation.

The above studies have helped to build a general knowledge of the odontocete ears, but comparative data are still lacking to relate the anatomy of hearing structures to species' acoustic characteristics.

All odontocetes recorded to date produce ultrasonic sounds and are assumed to echolocate (Au, 1993; Thomson & Richardson, 1995; Ketten, 2000). The recorded differences in echolocation signals are expected to reflect differences in hearing sensitivities supported by anatomical differences in auditory pathways. However, the coincidence between species-specific echolocation signals and hearing sensitivity has not yet been fully explored because of the difficulty of assessing the audiogram of wild individuals (Table 1).

The objective of this study was therefore to describe the ear of 15 odontocete species through computerized tomography scan 3D reconstructions and propose a set of standard measurements to be used to further assess their relationship to species' hearing sensitivity.

MATERIALS AND METHODS

To conduct a comparative analysis of the odontocete ear morphology, we used a diagnosis image method through computerized tomography (CT). Amongst other advantages, CT is a non-invasive technique and allows the information, obtained in a series of slices, to be further rendered in 3D. Images were stored in Hounsfield units, allowing a mapping of tissue densities via phantom calibration.

Computerized tomography scans of the tympanic-periotic (T-P) complex of 15 odontocete species were performed using the Siemens Somatom Emotion Duo. Sixty-nine ears from 45 stranded odontocetes from the Spanish and French

https://doi.org/10.1017/S0025315407054835 Published online by Cambridge University Press

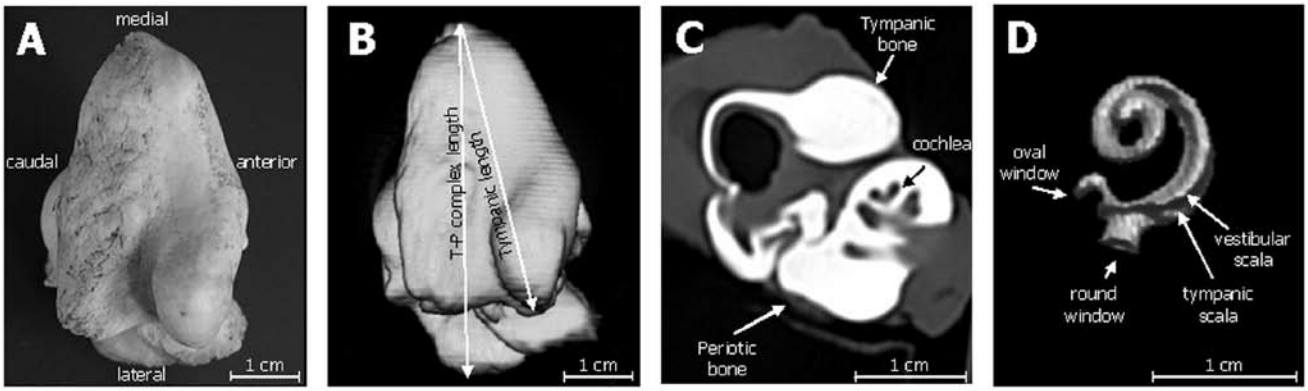

Figure 2. (A) Photograph of the ventral view left ear of a *Tursiops truncatus*; (B) T-P complex total length and tympanic length measurements from the rendered 3D volume of the same ear as in (A). The periotic length was also measured using the same methodology; (C) image obtained through CT scan of a *Tursiops truncatus* right ear; (D) 3D rendered cochlea of a *Steno bredanensis*.

North Atlantic and the Mediterranean Sea were extracted and preserved in formalin or kept dried after removal of soft tissues. Specifically, we analysed the T-P complex of *Tursiops truncatus* (12), *Stenella coeruleoalba* (10), *Stenella frontalis* (12), *Steno bredanensis* (2), *Delphinus delphis* (8), *Globicephala melas* (5), *Globicephala macrorhynchus* (2), *Lagenodelphis hosei* (2), *Kogia breviceps* (1), *Kogia simus* (2 periotic bones), *Physeter macrocephalus* (1 T-P and 1 periotic bone), *Phocoena phocoena* (7), *Ziphius cavirostris* (1), *Mesoplodon europaeus* (1) and *Mesoplodon densirostris* (1).

Following a standardized protocol, the samples were scanned in the same orientation in a helicoidal CT with spiral image acquisition, 130 kV voltage, 200 mA/s exposure, 760 projections every 360° for each slice, 1 mm section thickness with a reconstruction advance of 0.5 mm and resolution of 512 × 512 pixels (being the pixel size 0.1269 × 0.1269 mm^2).

To systematically orientate the T-P complex in the same position three reference points were dye-marked at the ear surface, two on the periotic and one on the tympanic, as can be seen in Figure 1.

The images were stored in digital imaging and communication in medicine (DICOM) format, processed using the computer 3D rendering software Analyze® 5.0 and presented with the 3D image viewer MRIcro® and Adobe Photoshop®.

The T-P complex volume, the Periotic (P) volume, the Tympanic (T) volume, the cochlear volume and the main lengths of both structures were measured using 3D tools in Analyze® 5.0.

Analyze® is a multidimensional image processing, visualization and analysis software that interprets and translates the differences in tissue densities in grey scale intensities. Bone threshold intensity value was set to be 645 to obtain a better image contrast. Following a determined intensity range the volume of a targeted organ could therefore be calculated.

Working with volumes permitted rotating the reconstructed ears until reaching the best projection to measure any length. Analyze® allowed us to calculate the direct linear length between two points selected on the screen. The lengths were measured as shown in Figure 2: (1) T-P complex total length (maximum length between the tympanic medial end and the periotic lateral end); (2) tympanic total length (maximum length between the tympanic medial end and the tympanic latero-anterior end); and (3) periotic total length (maximum length between the periotic medial end and the periotic lateral end).

We chose two methods to statistically analyse the data:

— the linear correlation coefficients to compare the relationship between all double combinations of measurements;

— the Fisher's discriminant analysis, a multivariant test which allows a comparison of all measurements together and classification of the species by these measurements. The power of discrimination (i.e. the weight) of each variable was calculated with the Fisher discriminant ratio comparing the species which contained a larger number of replicates (*T. truncatus*, *S. coeruleoalba*, *D. delphis*, *P. phocoena* and *S. frontalis*).

All the statistical tests and mathematical analysis were performed with the SPSS® software package, Matlab® 7.0 and Microsoft Excel®.

To assess the effect of age and because the species had different sizes, the statistical analysis was performed for the situations detailed in Table 2.

Mean and standard deviation estimates were calculated for each variable, giving a basis to build species-specific standard morphological measurements.

Table 2. *Specification of the four situations considered to compare the samples. All data were typified* ($[value - \overline{x}]/\sigma$).

Situation	Specification
1	only the adults typified data
2	only the adult data normalized by the animal length
3	adults and juveniles typified data
4	adult and juvenile data normalized by the animal length

RESULTS AND DISCUSSION

Linear correlation coefficients

The correlation coefficients between measurements were calculated for all animals (situation 3, Table 2) as well as for the adults separately (situation 1, Table 2). The results are shown in Table 3. The results obtained with adults were very

https://doi.org/10.1017/S0025315407054835 Published online by Cambridge University Press

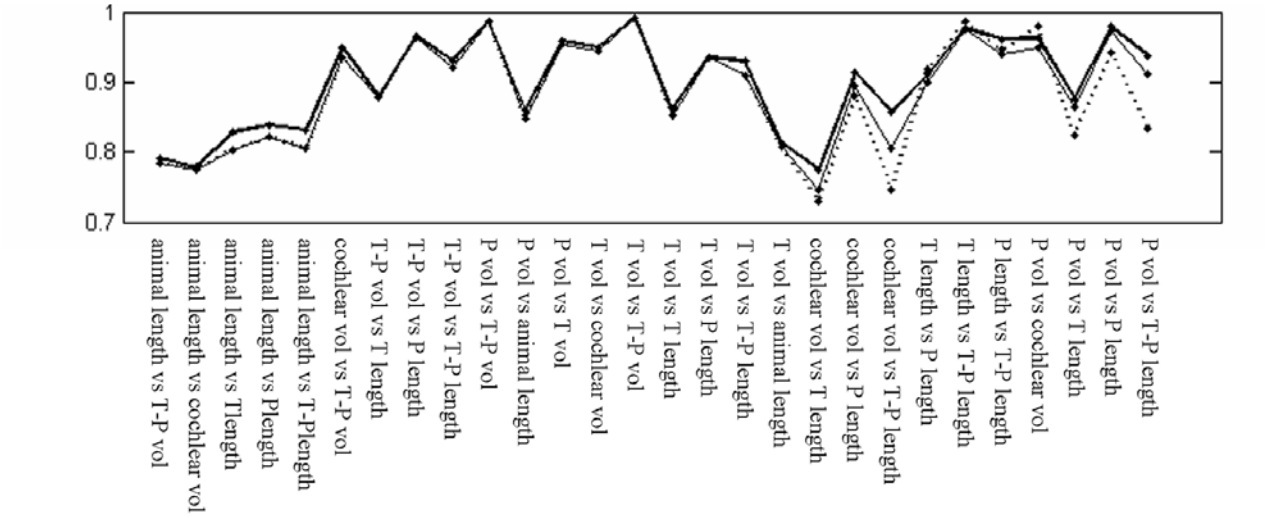

Figure 3. Representation of the correlation coefficients for the adults (thick line), all the data with the juveniles (dotted line) and all the data without the sperm whales, *Physeter macrocephalus* (thin line), between the two pairs of variables detailed on the x axis (see Table 3).

similar to those obtained when juveniles were also taken into account (Figure 3 and Table 3B).

When compared with other species, *P. macrocephalus* measurements showed greatest separation from the regression line, for the correlation coefficients were again calculated without taking into account this species. As shown in Figure 3, juveniles and adults together without *P. macrocephalus* gave a closer approximation to the values obtained with adults only, suggesting that the apparent differences in the coefficients between adults and juveniles could be due to the presence of *P. macrocephalus* in juvenile data.

All measurements were highly correlated (r >0.9) except in two scenarios:

— correlation was lower when comparing the animal length with the rest of the measurements (0.77< r <0.86);

— as for the cochlear volume, it proved to be highly related to all volumes and P lengths and to a lesser extent to all other lengths.

For all species the proportion between the tympanic and periotic bones appeared to remain constant meaning that any change in either structure (tympanic or periotic) is reflected in the other in the same proportion both in juveniles and adults. This constant ratio could be an indication of an existent

Table 3. *Correlation coefficients between measurements done in: (A) situation 3 and (B) situation 1 (see Table 2).*

(A)	T-P vol	Cochlear vol	P vol	T vol	T length	P length	T-P length	Animal length
T-P vol	1							
Cochl vol	0.934 (N=62)	1						
P vol	0.986 (N=35)	0.979 (N=39)	1					
T vol	0.991 (N=34)	0.945 (N=34)	0.955 (N=35)	1				
T length	0.878 (N=64)	0.730 (N=64)	0.825 (N=37)	0.853 (N=34)	1			
P length	0.964 (N=64)	0.881 (N=66)	0.941 (N=39)	0.935 (N=34)	0.918 (N=69)	1		
T-P length	0.922 (N=62)	0.745 (N=62)	0.834 (N=35)	0.910 (N=33)	0.986 (N=67)	0.946 (N=67)	1	
Animal length	0.785 (N=62)	0.775 (N=60)	0.847 (N=34)	0.807 (N=33)	0.803 (N=63)	0.821 (N=63)	0.805 (N=61)	1

(B)	T-P vol	Cochlear vol	P vol	T vol	T length	P length	T-P length	Animal length
T-P vol	1							
Cochl vol	0.950 (N=47)	1						
P vol	0.987 (N= 27)	0.963 (N=27)	1					
T vol	0.992 (N=26)	0.950 (N=26)	0.959 (N=26)	1				
T length	0.879 (N=47)	0.775 (N=47)	0.875 (N=27)	0.861 (N=26)	1			
P length	0.965 (N=47)	0.913 (N=47)	0.979 (N=27)	0.936 (N=26)	0.911 (N=47)	1		
T-P length	0.931 (N=45)	0.858 (N=45)	0.938 (N=25)	0.930 (N=25)	0.977 (N=45)	0.962 (N=45)	1	
Animal length	0.792 (N=47)	0.778 (N=47)	0.859 (N=27)	0.813 (N=26)	0.828 (N=47)	0.839 (N=47)	0.832 (N=45)	1

https://doi.org/10.1017/S0025315407054835 Published online by Cambridge University Press

Table 4. *Comparative results of the Fisher discriminant analysis for the 4 situations (see Table 2). The Fisher discriminant ratios for every variable are shown in columns 1 to 6. The maximum values for every situation are indicated in bold letters. Column 7 specifies the number of bad classified samples. Columns 8 and 9 reflect the percentage of variance for the two first functions while column 10 shows the Wilks' λ values.*

(A) Tt Sc Dd Pp Sf	1 T-P vol	2 Cochlear vol	3 T length	4 P length	5 T-P length	6 An. length	7 Bc	8 Function 1	8 Function 2	10 Wilks' λ
Situation 1 (N= 39)	46.1	25.9	77.1	80.2	87.8	**119.3**	1	92.9	5.3	0.002
Situation 2 (N= 39)	17.8	15.9	40.6	35.7	**61.9**		1	88.1	8.6	0.005
Situation 3 (N= 49)	48.0	29.2	72.3	**77.2**	75.1	27.2	4	83.7	11.5	0.009
Situation 4 (N= 49)	6.9	4.9	9.2	9.4	**11.2**		6	61.0	29.6	0.032
(B) All data										
Situation 1 (N=47)							1	93.6	4.9	0.000
Situation 2 (N=47)							1	91.7	4.8	0.000
Situation 3 (N=58)							3	79.1	14.2	0.000
Situation 4 (N=58)							14	74.0	13.4	0.003
(C)All data (classified by Types I and II)										
Situation 1 (N=47)							5	100	—	0.744
Situation 2 (N=47)							1	100	—	0.511
Situation 3 (N=58)							11	100	—	0.734
Situation 4 (N=58)							2	100	—	0.546

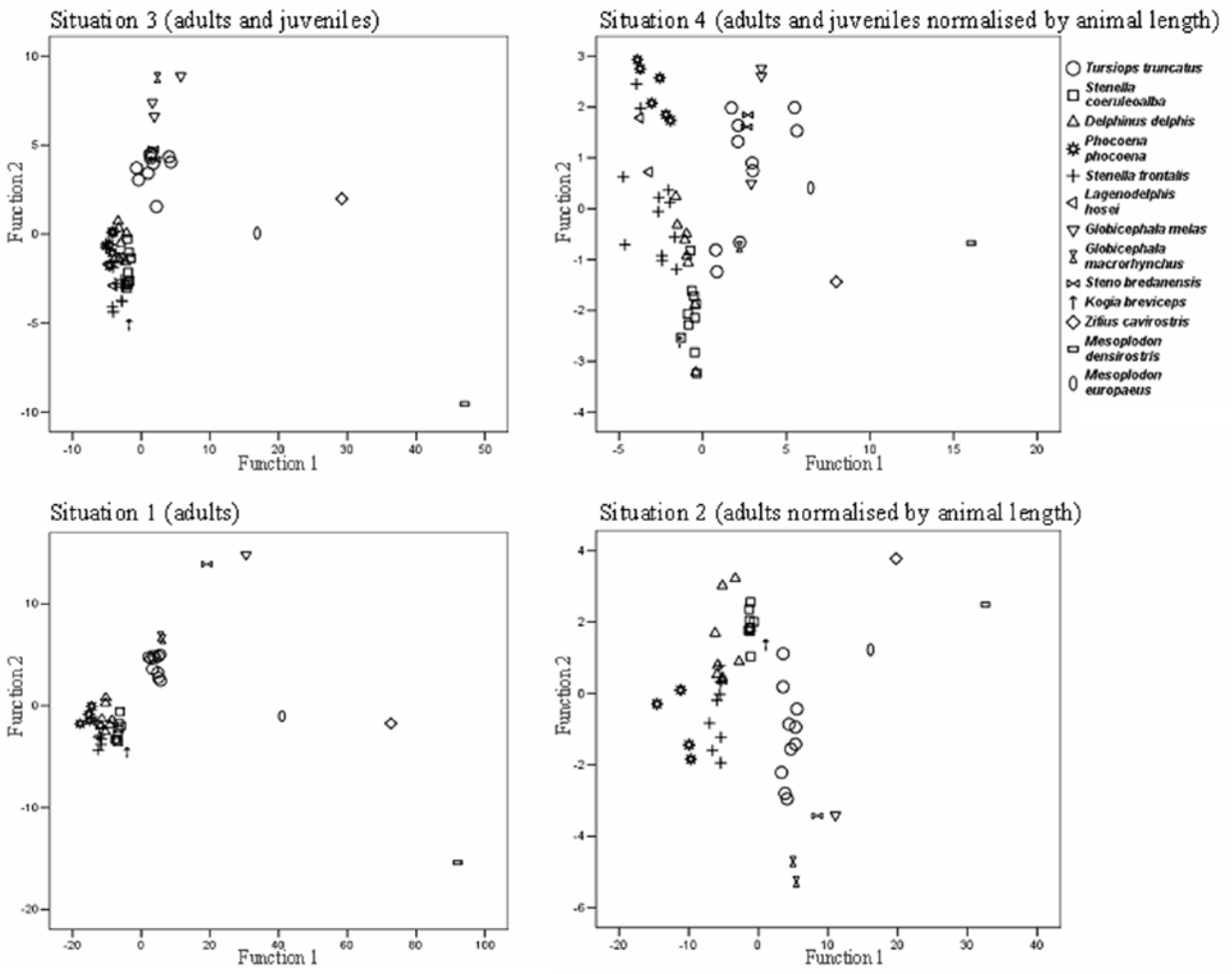

Figure 4. Plot of the 13 species in the two most discriminating projected dimensions (functions 1 and 2) resulting from the Fisher discriminant analysis for the four situations.

https://doi.org/10.1017/S0025315407054835 Published online by Cambridge University Press

Table 5. *Results summary.*

Test	Objectives	Results
Linear correlation coefficient	Compare one to one all double combinations of measurements	Very high correlations $0.9 < r < 0.99$ (except animal length with the rest of measurements and cochlear volume with some lengths) Adults and juveniles lead to similar results Without *Physeter macrocephalus* the coefficients are higher
Fisher discriminant analysis	Compare all the variables together to use all the available information from the measurements. Determine the weight of each variable	The measurements classify well the species. There is a strong dependency between the variables When juveniles are taken into acount the number of errors in the classification increases

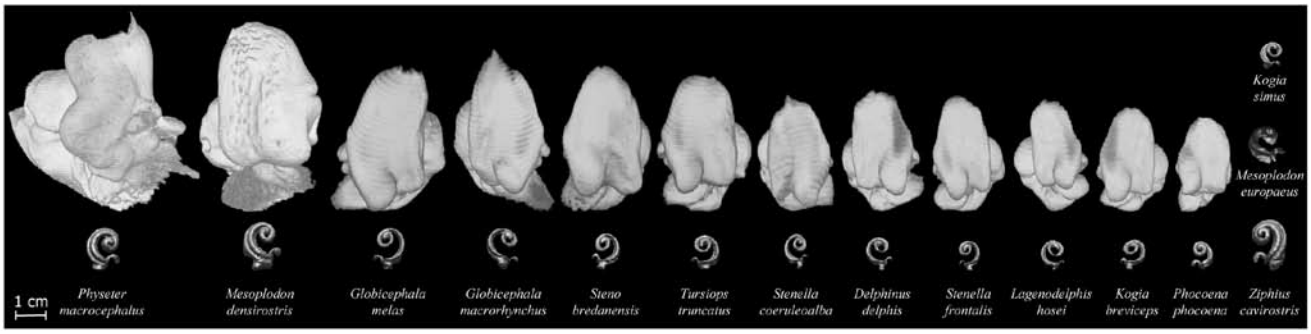

	T-P volume	Cochlear volume	P volume	T volume	T length	P length	T-P length	Animal length
Physeter macrocephalus	–	858.570* (σ= –)	26975.60* (σ= –)	–	56.143* (σ=0.650)	62.163* (σ=1.121)	67.785* (σ=5.593)	–
Mesoplodon densirostris	37013.470 (σ= –)	496.660 (σ= –)	16029.270 (σ= –)	20984.170 (σ= –)	53.096 (σ= –)	55.161 (σ= –)	65.016 (σ= –)	4350.0 (σ= –)
Ziphius cavirostris	27268.120 (σ= –)	410.410 (σ= –)	14553.250 (σ= –)	12714.820 (σ= –)	50.258 (σ= –)	56.706 (σ= –)	63.522 (σ= –)	5640.0 (σ= –)
Mesoplodon europaeus	18917.780 (σ= –)	281.610 (σ= –)	8232.270 (σ= –)	10685.510 (σ= –)	41.847 (σ= –)	43.910 (σ= –)	53.909 (σ= –)	4090.0 (σ= –)
Globicephala melas	13668.135 (σ=1326.624)	184.035 (σ= 9.256)	6526.550 (σ= –)	6550.990* (σ=50.883)	45.651 (σ= 3.164)	39.138 (σ= 0.929)	55.651 (σ= –)	4550.0 (σ= 353.553)
Globicephala macrorhynchus	12956.460 (σ= 159.651)	141.445 (σ= 0.262)	6280.615 (σ= 18.576)	6675.845 (σ=141.075)	48.187 (σ= 0.035)	38.581 (σ= 0.264)	52.726 (σ= –)	3650.0 (σ= –)
Steno bredanensis	12032.470 (σ= 21.510)	100.780 (σ= 0.636)	5704.085 (σ= 22.253)	6328.385 (σ= 0.742)	41.846 (σ= 0.212)	36.562 (σ= 0.559)	48.842 (σ= 0.260)	2470.0 (σ= –)
Tursiops truncatus	11019.790 (σ=1802.143)	141.070 (σ= 21.243)	5161.973 (σ= 82.305)	6198.823 (σ=494.443)	39.831 (σ= 1.474)	37.203 (σ= 1.532)	47.703 (σ= 2.127)	2457.5 (σ= 355.075)
Stenella coeruleoalba	6211.381 (σ= 641.363)	88.561 (σ= 14.437)	3830.160 (σ= 66.059)	3049.740 (σ= 27.279)	32.998 (σ= 1.358)	31.136 (σ= 1.264)	37.801 (σ= 1.166)	2207.8 (σ= 27.739)
Delphinus delphis	5910.505 (σ= 565.997)	106.193 (σ= 16.841)	3350.373 (σ=442.168)	2973.750 (σ=339.864)	33.353 (σ= 1.153)	30.383 (σ= 1.709)	38.779 (σ= 0.962)	1827.5 (σ= 138.538)
Stenella frontalis	5156.086 (σ= 367.356)	65.693 (σ= 6.142)	2653.413 (σ=109.811)	2346.935 (σ=158.500)	31.277 (σ= 0.905)	28.402 (σ= 0.392)	36.301 (σ= 0.595)	1792.5 (σ= 73.046)
Lagenodelphis hosei	5053.050* (σ=21.185)	59.250* (σ=3.224)	3079.800* (σ=14.835)	1973.250* (σ=6.350)	29.335* (σ=0.505)	30.387* (σ=0.033)	36.538* (σ=0.676)	1300.0* (σ= –)
Kogia breviceps	4748.620 (σ= –)	72.770 (σ= –)	2470.950 (σ= –)	2277.670 (σ= –)	30.539 (σ= –)	27.929 (σ= –)	33.922 (σ= –)	2580.0 (σ= –)
Kogia simus	–	57.620* (σ=1.527)	2311.965* (σ=1.011)	–	–	25.444* (σ=0.016)	–	–
Phocoena phocoena	5486.483 (σ= 235.367)	83.565 (σ= 11.348)	2050.025 (σ=88.028)	3475.590 (σ=124.875)	31.883 (σ= 0.848)	29.655 (σ= 0.565)	38.801 (σ= 0.646)	1477.5 (σ= 95.000)

Figure 5. Macroscopical on scale 3D reconstructions of all the species rendered bullae and cochlear volumes. The rendered T-P volume was not shown when the complete T-P complex was not available (either T or P were missing). The above table shows the means and standard deviations of the adult variables, giving a basis to build species-specific standard morphological measurements. All the volumes were presented in mm^3 and all the lengths in mm. The values marked with * were calculated from juveniles.

https://doi.org/10.1017/S0025315407054835 Published online by Cambridge University Press

functionality between both structures, supporting an active role of the middle ear in the odontocete sound reception mechanism as suggested by recent modelling analysis (Nummela et al., 1999a, 1999b; Hemilä et al., 1999, 2001).

Our results are generally consistent with previous studies (Ketten, 1992), although here the correlation coefficients between animal lengths and the total volume and lengths of the bullae, are much lower (Ketten & Wartzok, 1990), indicating that the length of the animals may not be a primary parameter to take into account when defining ear measurements.

With this one dimensional statistical test we could not differentiate between all the species or calculate the weight of each variable to classify them. The results (see below) from a multi-discriminant analysis allowed us to find the most discriminant variables from our measurements.

Fisher discriminant analysis (FDA)

We first calculated the individual variables discriminant power with Fisher's discriminant ratios. To make the analysis more robust, ratios were only evaluated for the five species presenting more replicates, mentioned above (*T. truncatus*, *S. coeruleoalba*, *D. delphis*, *P. phocoena* and *S. frontalis*). These ratios, which give the weight of the variables — a higher ratio means a stronger discriminant power — are presented in columns 1 to 6, Table 4A. In all four situations (Table 2), the cochlear volume appeared to be the variable with the lowest weight. Additionally, in situation 3 the animal length also seemed to have little importance despite being a strong discriminator in situation 1. This difference can be explained by the fact that these species present different lengths and that juveniles from a species could easily be misclassified as an adult from a smaller species. The variable that generally displayed the strongest discriminant power was the T-P complex length.

Next, we performed a FDA on the combination of all variables (Figure 4). The four plots show classification results in the four different situations (Table 2). The classification errors are listed in column 7 of Table 4. When juveniles are taken into account the number of misclassifications increases. This would indicate that morphological changes of the ear are not linearly related to animal growth.

In Table 4, function 1 and function 2 are the two most discriminant projected dimensions resulting from FDA. Table values reflect the percentage of the data variability. Since most of the variability is explained by the two first functions, we can assume that there is strong dependency between the variables.

The last column in the table shows the Wilks' λ: a very low value would indicate that the means of the classes are well separated, which is the case here (Table 4A and 4B). These results confirm that all combined variables classify the species very well.

Because the results for adults and juveniles did not lead to the same relationship between variables, we used adults for standard ear mean and standard deviation calculations. In cases when we had no adults, juveniles were used. Figure 5 shows these values as species-specific standard measurements, as well as the scale reconstructions of all the T-P complex and cochlea volumes.

Ketten & Wartzok (1990) and Ketten (1992, 1994) divided the odontocete ears into two Types: I and II, depending on click peak frequency production. In our study there is just one type I species, *P. phocoena* (which presents a peak frequency >100 kHz), the rest of the species being all of type II. When conducting the FDA considering these two types, some Type II individuals were misclassified as Type I (see column 7, Table 4C), which is not consistent with the Ketten & Wartzok results (1990). The high Wilks' λ values presented in Table 4C support the fact that the variables do not classify well between Type I and II species. In addition, their analysis compared ear anatomy with sound production while our study aimed at focusing on the relationship between sound reception sensitivity and hearing structures. Unfortunately, there is still a great need for data on species-specific audiograms (Table 1) as well as individual hearing measurements within the same species, before we can statistically explore the above dependence under a multi-dimensional analysis. Electrophysiological measures of hearing appear the most promising source of data. Table 5 shows a summary of the results obtained with the two statistical tests.

CONCLUSION

Being a non-invasive technique and supporting a very high resolution in 3D reconstructions, computerized tomography is confirmed to be a powerful tool for the study of the tympanic-periotic complex morphology and morphometry, leading to close-to-reality results.

The apparent functional relationship between the periotic and tympanic bullae suggested by the constant ratio between measurements added some information on the role of the odontocete middle ear during target acoustic detection.

The analysis showed that the odontocete ear morphometrics is a good species indicator and could therefore be used to classify them. It also suggests that the described measurements can characterize standard ears and may therefore constitute a morphological basis for further species-specific acoustic comparison.

This study was funded by the BBVA foundation. The analysis was conducted with the collaboration of the Hospital Clinic de Barcelona and the Centro de Asistencia a la Investigación de la Universidad Complutense de Madrid. We are grateful to the staff of Dr Concepció Bru from the Hospital Clinic, especially Dr Carles Falcon and Dra Núria Bargalló for their time and dedication.

REFERENCES

Au, W.W.L., 1993. *The sonar of dolphins*. New York: Springer-Verlag.

Awbrey, F.T., Thomas, J.A. & Kastelein, R.A., 1988. Low-frequency underwater hearing sensitivity in Belugas, *Delphinapterus leucas*. *Journal of the Acoustical Society of America*, **84**, 2273–2275.

Bullock, T.H. et al., 1968. Electrophysiological studies of central auditory mechanisms in cetaceans. *Zeitschrift für vergleichende Physiologie*, **59**, 117–156.

Fleischer, G., 1978. Evolutionary principles of the mammalian middle ear. *Advances in Anatomy, Embryology and Cell Biology*, **55**, 1–70.

Fraser, F.C. & Purves, P.E., 1954. Hearing in cetaceans. *Bulletin of the British Museum (Natural History) Zoology*, **2**, 103–116.

Fraser, F.C. & Purves, P.E., 1960. Hearing in cetaceans. Evolution of the accessory air sacs and the structure and function of the outer and middle ear in recent cetaceans. *Bulletin of the British Museum (Natural History) Zoology*, **7**, 1–140.

Hall, J.D. & Johnson, C.S., 1971. Auditory thresholds of a killer whale *Orcinus orca* Linnaeus. *Journal of the Acoustical Society of America*, **51**, 515–517.

Hemilä, S., Nummela, S. & Reuter, T., 1999. A model of the odontocete middle ear. *Hearing Research*, **133**, 82–97.

Hemilä, S., Nummela, S. & Reuter, T., 2001. Modeling whale audiograms: effects of bone mass on high-frequency hearing. *Hearing Research*, **151**, 221–226.

Jacobs, D.W. & Hall, J.D., 1972. Auditory thresholds of a fresh water dolphin, *Inia geoffrensis* Blainville. *Journal of the Acoustical Society of America*, **51**, 530–533.

Johnson, C.S., 1967. Sound detection thresholds in marine mammals. In *Marine bioacoustics* (ed. W.N. Tavolga), pp. 247–260. New York: Pergamon Press.

Johnson, C.S., 1992. Detection of tone glides by the beluga whale. In *Marine mammal sensory systems* (ed. J.A. Thomas et al.), pp. 241–247. New York: Plenum Press.

Kastelein, R.A., Bunskoek, P., Hagedoorn, M., Au, W.W.L. & de Haan, D., 2002. Audiogram of a harbor porpoise (*Phocoena phocoena*) measured with narrow-band frequency-modulated signals. *Journal of the Acoustical Society of America*, **112**, 334–344.

Kastelein, R.A., Hagedoorn, M., Au, W.W.L. & de Haan, D., 2003. Audiogram of a striped dolphin (*Stenella coeruleoalba*). *Journal of the Acoustical Society of America*, **113**, 1130–1137.

Ketten, D., 1992. The cetacean ear: form, frequency and evolution. In *Marine mammal sensory systems* (ed. J.A. Thomas et al.), pp. 56–69. New York: Plenum Press.

Ketten, D.R., 1994. Functional analyses of whale ears: adaptations for underwater hearing. *Oceans' 94 Proceedings*, 264–270.

Ketten, D.R. & Wartzok, D., 1990. Three-dimensional reconstructions of the dolphin ear. In *Sensory abilities of cetaceans* (ed. J. Thomas and R. Kastelein), pp. 81–105. New York: Plenum Press.

Ketten, D., 2000. Cetacean ears. In *Hearing by whales and dolphins* (ed. W.W.L. Au et al.), Springer handbook of auditory research, pp. 43–108. New York: Springer-Verlag.

Klishin, V.O., Popov, V.V. & Supin, A. Ya., 2000. Hearing capabilities of a beluga whale. *Aquatic Mammals*, **26**, 212–228.

Ljungblad, D.K., Scoggins, P.D. & Gilmartin, W.G., 1982. Auditory thresholds of a captive eastern Pacific bottlenosed dolphin *Tursiops* spp. *Journal of the Acoustical Society of America*, **72**, 1726–1729.

McCormick, J.G., Wever, E.G., Palin, J. & Ridgway, S.H., 1970. Sound conduction in the dolphin ear. *Journal of the Acoustical Society of America*, **48**, 1418–1428.

Nachtigall, P.E., Au, W.W.L., Pawloski, J.L. & Moore, P.W.B., 1995. Risso's dolphin (*Grampus griseus*) hearing thresholds in Kaneohe Bay, Hawaii. In *Sensory systems of aquatic mammals* (ed. R.A. Kastelein et al.), pp. 49–54. Woerden: DeSpill Publishers.

Nummela, S., Wagar, T., Hemilä, S. & Reuter, T., 1999a. Scaling of the cetacean middle ear. *Hearing Research*, **133**, 71–81.

Nummela, S., Reuter, T., Hemilä, S., Holmberg, P. & Paukku, P., 1999b. The anatomy of the killer whale middle ear (*Orcinus orca*). *Hearing Research*, **133**, 61–70.

Popov, V.V., Ladygina, T.F. & Supin, A. Ya., 1986. Evoked potentials in the auditory cortex of the porpoise, *Phocoena phocoena*. *Journal of Comparative Physiology A*, **158**, 705–711.

Popov, V.V. & Supin, A. Ya., 1987. White whale (*Delphinapterus leucas*) hearing characteristics. *Doklady Akademii Nauk Sssr*, **294**, 1255–1258.

Popov, V.V. & Supin, A. Ya., 1990a. Auditory brain-stem responses in characterization of dolphin hearing. *Journal of Comparative Physiology A*, **166**, 385–393.

Popov, V.V. & Supin, A. Ya., 1990b. Electrophysiological study of hearing in the fresh-water dolphin, *Inia Geoffrensis*. *Doklady Akademii Nauk Sssr*, **313**, 238–241.

Popov, V.V. & Klishin, V.O., 1998. EEG study of hearing in the common dolphin, *Delphinus delphis*. *Aquatic Mammals*, **24**, 13–20.

Reysenbach de Haan, F.W., 1957. Hearing in whales. *Acta Otolaryngolica*, Suppl, **134**, 1–114.

Ridgway, S.H., 1983. Dolphin hearing and sound production in health and illness In *Hearing and other senses* (ed. Presentations in honor of E.G. Wever, R.R. Fay and G. Gourevitch), p. 405. Box N, Groton, CT 06340. The Amphora Press, xii.

Ridgway, S.H, Carder, D., Smith, R., Kamolnick, T. & Elsberry, W., 1997. First audiogram for marine mammals in the open ocean and at depth: hearing and whistling by two white whales down to 30 atmospheres. *Journal of the Acoustical Society of America*, **101**, 3136.

Sauerland, M. & Dehnhardt, G., 1998. Underwater audiogram of a tucuxi (*Sotalia fluviatilis guianensis*). *Journal of the Acoustical Society of America*, **103**, 1199–1204.

Szymanski, M.D., Bain, D.E., Kiehl, K., Pennington, S., Wong, S. & Henry, K.R., 1999. Killer whale (*Orcinus orca*) hearing: auditory brainstem response and behavioral audiograms. *Journal of the Acoustical Society of America*, **106**, 1134–1141.

Thomas, J., Chun, N., Au, W. & Pugh, K., 1988. Underwater audiogram of a false killer whale (*Pseudorca crassidens*). *Journal of the Acoustical Society of America*, **84**, 936–940.

Thomson, D.H. & Richardson, W.J., 1995. Marine mammal sounds. In *Marine mammals and noise* (ed. W.J. Richardson et al.), pp. 182–183. San Diego: Academic Press.

Tremel, D.P., Thomas, J.A., Ramirez, K.T., Dye, G.S., Bachman, W.A., Orban, A.N. & Grimm, K.K., 1998. Underwater hearing sensitivity of a Pacific white-sided dolphin, *Lagenorhinchus obliquidens*. *Aquatic Mammals*, ***24***, 63–69.

Wang, D., Wang, K.X., Xiao, Y. & Sheng, G., 1992. Auditory sensitivity of a Chinese river dolphin, *Lipotes vexillifer*. In *Marine mammal sensory systems* (ed. J.A. Thomas et al.), pp. 213–222. New York: Plenum press.

Wever, E.G., McCormic, J.G., Palin, J. & Ridgway, S.H., 1971a. Cochlea of dolphin, *Tursiops truncatus* — general morphology. *Proceedings of the National Academy of Sciences of the United States of America*, **68**, 2381–2385.

Wever, E.G., McCormic, J.G., Palin, J. & Ridgway, S.H., 1971b. Cochlea of dolphin, *Tursiops truncatus*. 2. Basilar membrane. *Proceedings of the National Academy of Sciences of the United States of America*, **68**, 2708–2711.

Wever, E.G., McCormic, J.G., Palin, J. & Ridgway, S.H., 1971c. Cochlea of dolphin .3. *Tursiops truncatus* — Hair cells and ganglion cells. *Proceedings of the National Academy of Sciences of the United States of America*, **68**, 2908–2912.

White, M.J.J., Norris, J.C., Ljungblad, D.K., Baron, K. & di Sciara, G., 1978. Auditory thresholds of two belugas whales (*Delphinapterus leucas*) In: *Hubbs Sea World Research Institute Technical Report*, 78–109. San Diego, CA: Hubbs Sea World Marine Research Institute.

Submitted 15 June 2006. Accepted 25 October 2006.